

Effects of Spring Biomass Burning in the Indochina Peninsula on May Precipitation in South China

Qianqian Mao, Shuyu Liu, Yu Huang

School of Atmospheric Sciences, Nanjing University of Information Science and Technology, Nanjing, China

Email: mq131366@163.com

How to cite this paper: Mao, Q.Q., Liu, S.Y. and Huang, Y. (2023) Effects of Spring Biomass Burning in the Indochina Peninsula on May Precipitation in South China. *Journal of Water Resource and Protection*, 15, 179-193.

<https://doi.org/10.4236/jwarp.2023.155011>

Received: April 17, 2023

Accepted: May 8, 2023

Published: May 11, 2023

Copyright © 2023 by author(s) and Scientific Research Publishing Inc.

This work is licensed under the Creative Commons Attribution International License (CC BY 4.0).

<http://creativecommons.org/licenses/by/4.0/>



Open Access

Abstract

Each year, during the dry season that precedes the summer wind and rainfall Indo-China Peninsula (ICP), significant biomass burning occurs and reaches its peak from March to April. This biomass burning generates large amounts of aerosols that impact East Asia and surrounding areas through the Asian monsoon. This study aims to investigate the potential connection between biomass burning over the ICP and precipitation in South China during May, along with the physical processes involved. The analysis is based on GLDAS soil moisture reanalysis data and CPC (NOAA) precipitation data covering the period from 1980 to 2021. The research findings indicate a negative (positive) correlation between biomass burning in the ICP region during spring and precipitation in the same region (South China) during May. The circulation patterns corresponding to years with biomass-burning emission anomalies are further investigated, and the impact of biomass-burning emissions in spring on soil moisture and temperature is examined. The results suggest that biomass-burning emissions can significantly affect atmospheric circulation and precipitation, ultimately leading to anomalous precipitation in South China.

Keywords

Indo-China Peninsula, Biomass-Burning Aerosols, Atmospheric Circulation, Precipitation

1. Introduction

The ICP is considered one of the most severely affected regions in Asia due to biomass burning. According to satellite monitoring, the Southeast Asian area witnesses over 20,000 ignition points each spring [1]. Biomass-burning emissions

result in significant amounts of aerosols, such as black carbon, organic carbon, and elemental carbon [2]. These aerosol particles have varying optical properties that determine their ability to absorb, scatter, and reflect radiation, thus regulating the radiative flux and energy balance of the atmosphere, ultimately affecting the climate system. This is commonly known as the aerosol direct or radiative effect [3]. Additionally, biomass-burning aerosols can cause atmospheric warming and surface cooling, leading to changes in atmospheric stability and cloud cover, which is referred to as the semi-direct effect of aerosols [4] [5]. Furthermore, these aerosols can also act as cloud condensation nuclei, altering cloud formation, and influencing other microphysical processes, also known as aerosol-cloud interactions [6] [7].

Biomass burning is a major source of aerosol emissions, primarily from forest or grassland fires, as well as straw burning due to human activities. These aerosols have significant impacts on the Earth-atmosphere system. Through their radiative effects, these emissions can alter the distribution of energy between the surface and atmosphere, resulting in modifications in the atmospheric thermodynamic structure and regulation of the water cycle. Consequently, they have significant implications for the monsoon circulation, and regional and global climate [8] [9]. The effects of biomass burning on the regional climate can be observed in various areas, including North America, Asia, and Africa. Forest fires in these regions can cause a significant decrease in surface temperature [10] [11] [12]. Furthermore, biomass-burning aerosols can inhibit cloud development by reducing surface temperature and increasing atmospheric stability [13] [14] [15], thereby suppressing precipitation [16]. In addition, they can even affect the occurrence and development of monsoons [17]. As [18] conducted a study that integrated ground observation data with regional modeling, revealing the significant impact of aerosols on shortwave radiation, sensible heat, and surface temperature. Consequently, these aerosols affect the short-term precipitation processes in local regions and play a crucial role in regional weather systems. [19] discovered that aerosols, stemming from biomass burning in Southeast Asia, can reduce early-season precipitation in East Asia by 40%. [20] suggested that biomass burning can inhibit convective precipitation during the day and enhance nocturnal precipitation.

In addition, aerosols can exert an extensive influence on East Asia and its surrounding regions via the Asian monsoon, even extending to the western Pacific area, as demonstrated by previous studies [21] [22]. [23] discovered that aerosols could lower the surface temperature by absorbing and radiating shortwave radiation, which weakens the land-sea temperature gradient over South Asia, the Indian Ocean, and the Bay of Bengal, thus affecting the Indian monsoon. Similarly, [24] found that anthropogenic aerosols weaken the circulation of the South Asian summer monsoon, while absorbing aerosols could enhance the western Pacific subtropical high and increase the transport of warm and moist air, causing decreased precipitation in southern China and increased precipitation in northern China [25]. Furthermore, atmospheric cir-

ulation models applied by [26] demonstrated that aerosols could intensify the vertical uplift motion over the northern Indian Ocean and the Indian subcontinent by heating the convective layer, leading to increased precipitation. Nevertheless, [27] pointed out that the impact of aerosols on precipitation is time-dependent.

Recent research has provided evidence that biomass burning in the Indochina Peninsula plays a vital role in the occurrence and development of the Asian monsoon, and the southern China region is a sensitive area for the outbreak of this monsoon. Moreover, early biomass burning in the Indochina Peninsula can have a substantial impact on the climate of the southern China region. However, despite its potential significance, there have been limited studies on the effects of spring biomass burning on precipitation in this area. Therefore, this study aims to investigate the possible correlations and associated mechanisms between anomalous biomass burning in the spring in the Indochina Peninsula and precipitation anomalies in southern China. The ultimate objective is to enhance our understanding of the changes in the East Asian summer monsoon and improve weather and climate forecasting in East Asia, which has significant practical implications. This study first analyzes the relationship between spring biomass burning in the Southeast Asia region and May precipitation in southern China. Subsequently, it investigates the mechanism by which spring biomass burning affects May precipitation in southern China, examining differences in atmospheric circulation, land-surface properties, and land-atmosphere energy transfer during anomalous years of spring biomass burning.

2. Data and Methods

2.1. Data

The precipitation data used in this study was obtained from the Global Unified Daily Quality-Controlled Precipitation Dataset, which was provided by the Climate Prediction Center (CPC) of the National Oceanic and Atmospheric Administration (NOAA) of the United States. This dataset has a high spatial resolution of $0.5^\circ \times 0.5^\circ$ and covers the time period from 1980 to 2021. The dataset is primarily derived from observations made by multiple sources, including satellites, meteorological stations, automated precipitation measurement systems, and ground-based precipitation observation stations. Such a diverse range of sources ensures the accuracy and reliability of the data used in this research.

As the availability of soil moisture observation data is limited, this study acquired soil moisture information from the monthly data generated by the Noah land surface model in the Global Land Data Assimilation System (GLDAS), which has a resolution of $0.25^\circ \times 0.25^\circ$ [28]. GLDAS is a global land data assimilation system, jointly developed by the Goddard Space Flight Center (GSFC) of the National Aeronautics and Space Administration (NASA) and the National Centers for Environmental Prediction (NCEP) of the National Oceanic and At-

mospheric Administration (NOAA). GLDAS employs advanced data assimilation techniques and modeling methods to process satellite and ground observation data products, integrates a large amount of observation data supported by the Land Information System (LIS), and obtains the optimal surface flux field, driving multiple surface process models. Widely used in weather forecasting, climate change, water cycle studies, and water resources applications, GLDAS-Noah model simulates four soil layers with a depth of 2 meters, and the thickness of each layer from top to bottom is 10 cm, 30 cm, 60 cm, and 100 cm, respectively [29]. This study chose the top 0 - 10 cm soil layer to represent the soil moisture information. Additionally, GLDASv2.0 and GLDASv2.1 were combined for the time periods of 1980-2014 and 2015-2020, respectively, to ensure consistency with other variables in the time series.

The study utilized monthly data from 1980 to 2021 of the potential height field, wind field, water vapor field, and surface temperature, all of which were obtained from the MERRA2 reanalysis dataset with a resolution of $0.5^\circ \times 0.625^\circ$. The MERRA2 reanalysis dataset is a comprehensive and rare set of reanalysis data that combines basic meteorological fields and atmospheric chemistry fields, such as aerosol emissions, concentrations, and optical thickness. This dataset is generated by the Goddard Earth Observing System Model, Version 5 (GEOS-5) atmospheric data assimilation system developed by NASA.

2.2. Methods

This study mainly employed commonly used statistical analysis methods in meteorology, including correlation analysis, synthesis analysis, and t-tests.

3. Results and Analysis

To investigate the spatiotemporal distribution of biomass burning in the ICP region, this study employed the MERRA2 reanalysis dataset to generate a spatial distribution map of aerosol optical thickness for East and Southeast Asia from 1980 to 2021, covering all 12 months of the year (Figure 1). The results demonstrate a significant increase in aerosol optical thickness over the ICP region, with a noticeable spike in spring, specifically during March and April. The South China Sea and southern China also exhibited high levels of aerosol optical thickness. Biomass burning in the ICP region primarily emits aerosols in the eastern and western parts of Myanmar, northern Laos, and the northwest of Thailand, as well as the northeastern part of India, while emissions in proximity to China are mainly concentrated in the eastern part of Myanmar and northern Laos. This spatiotemporal distribution pattern is consistent with prior research findings [30]. Biomass burning in the ICP region has the potential to affect the air quality and climate of downstream regions, particularly the South China Sea and Taiwan area, through the Asian monsoon [31] [32].

To better illustrate the atypical variations in biomass burning in the ICP region, this study focused on the area between $92^\circ\text{E} - 110^\circ\text{E}$ and $10^\circ\text{N} - 25^\circ\text{N}$ and

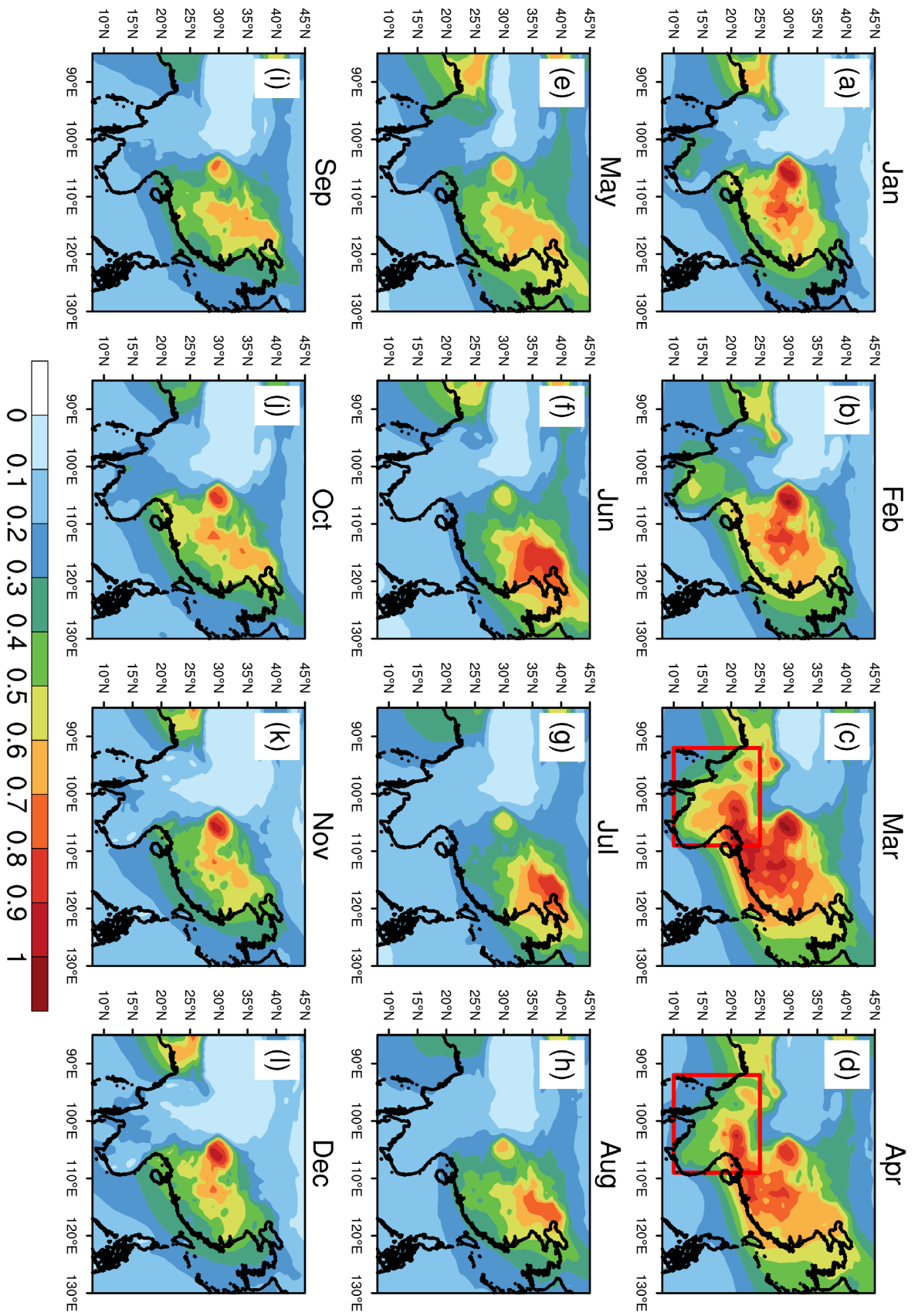


Figure 1. Spatial distribution of AOD by month for climate mean state.

calculated the average Aerosol Optical Thickness (AOT) during the spring months (March–April) from 1980 to 2021 (**Figure 1(c)**, **Figure 1(d)**). The data was standardized and represented as the biomass-burning Index (I_{AOD}), which reflects the inter-annual anomalous changes in biomass burning during the spring season in the ICP region, while accounting for any long-term trends. **Figure 2** presents the inter-annual variation of I_{AOD} between 1980 and 2021, highlighting a significant inter-annual variation in spring biomass burning in the ICP region. To facilitate subsequent analysis, years with I_{AOD} values greater than 0.8 were classified as years with anomalous high biomass burning (1982, 1983, 1992, 1998, 2004, 2010, 2012, 2014, 2016), whereas those with I_{AOD} values less than -0.8 were classified as years with anomalous low biomass burning (1988, 1989, 1994, 1996, 1997, 2001, 2002, 2017, 2018).

Figure 3(a) depicts the distribution of the I_{AOD} index for May precipitation, revealing a significant positive correlation between biomass burning in the ICP during spring and May precipitation in southern China. The results suggest that the increase in emissions from spring biomass burning over the ICP contributes to a corresponding increase in precipitation in May in southern China, whereas decreased emissions cause a reduction in precipitation. This can result in abnormal soil moisture levels, as noted in prior research [33].

To further explore this relationship, we calculated the standardized sequence of average soil moisture in the southern region of China during May from 1980–2021, defining it as the I_{SM} index for spring soil moisture. **Figure 3(b)** shows the distribution of the I_{SM} index for May precipitation, indicating a significant positive correlation between May precipitation and soil moisture in southern China. Thus, changes in precipitation can lead to abnormal soil moisture levels, with increased precipitation in May resulting in relatively moist soil and decreased precipitation leading to relatively dry soil. These results suggest that analyzing soil moisture data can accurately reflect the soil moisture status of a region to a certain extent and should be considered a reliable method for predicting

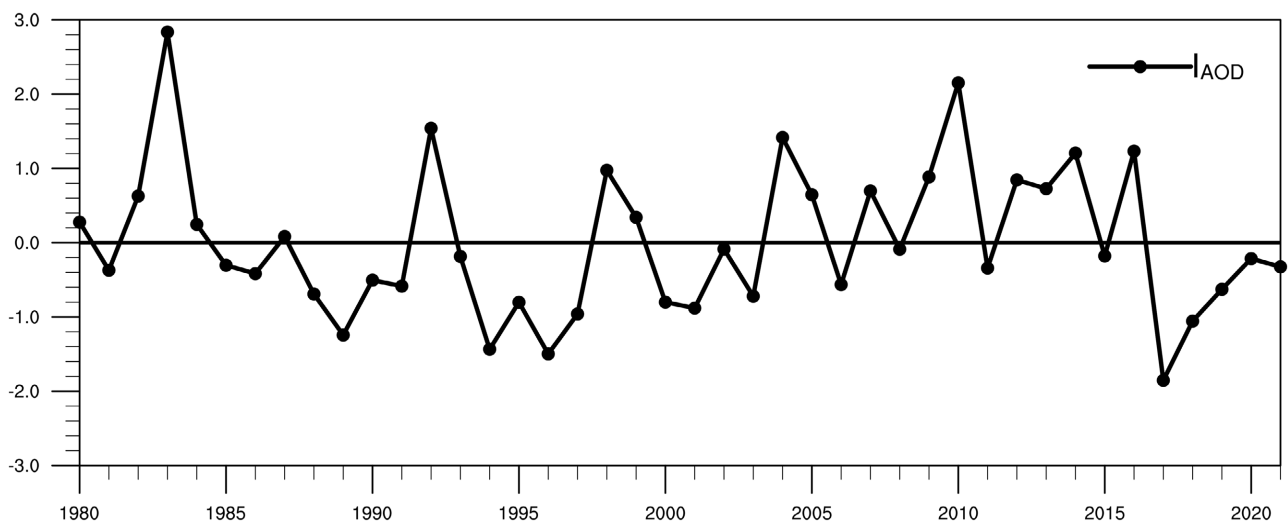


Figure 2. Interannual variation curve of springtime biomass-burning index I_{AOD} over the ICP.

precipitation and soil moisture levels.

To examine the anomalous May precipitation in the ICP region associated with spring biomass burning, this study conducted a composite analysis of May precipitation changes during years of anomalous high and low biomass burning, which were previously identified based on aerosol optical thickness. **Figure 4** displays the spatial distribution of the May precipitation anomaly composite between high and low biomass-burning years, showing that during years of

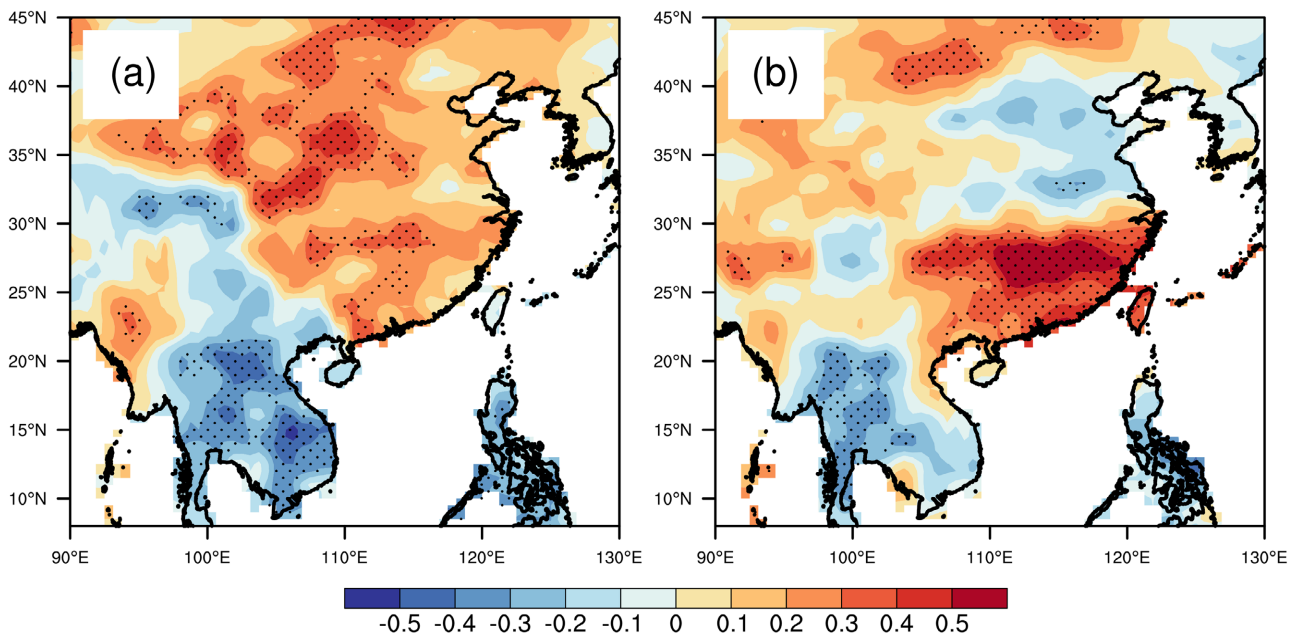


Figure 3. Correlation distribution of I_{AOD} index (a) with I_{SM} index (b) and May precipitation; hit points pass the significance test of 0.05.

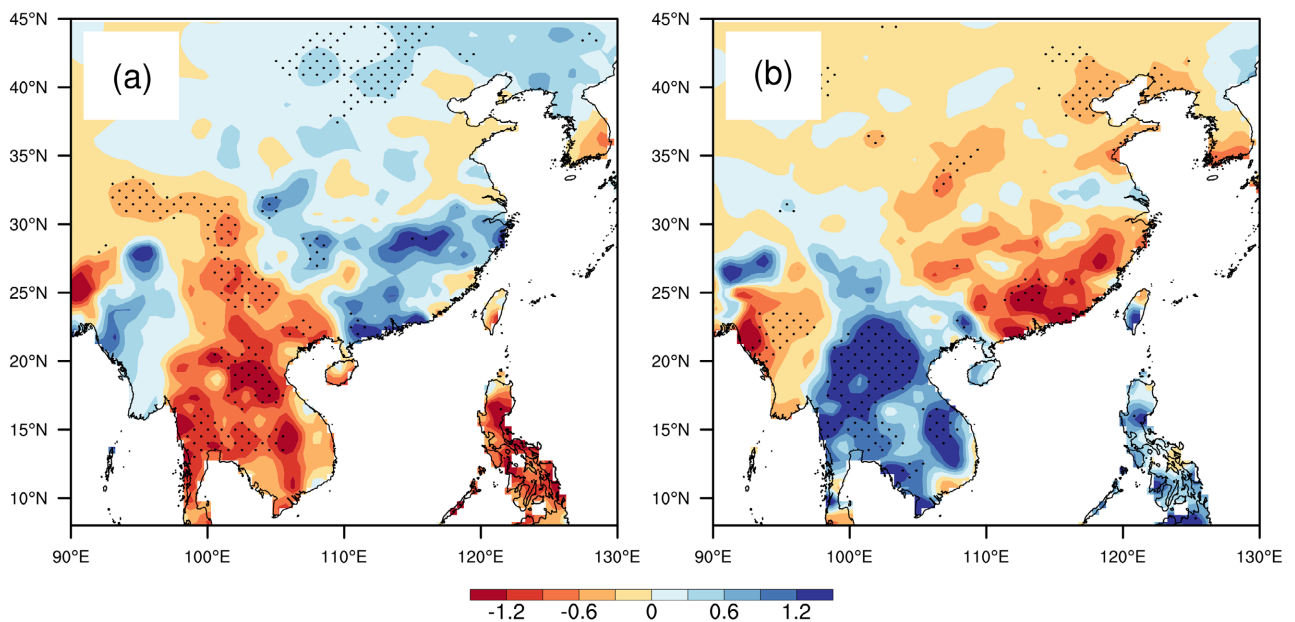


Figure 4. Synthetic field of May precipitation distance level (in mm/day): (a) high biomass combustion emission year; (b) low emission year; punctured area passes significance test of 0.05.

anomalous high biomass burning, May precipitation in the ICP region exhibited a negative anomaly, indicating a significant deviation from normal conditions, while precipitation in southern China displayed a positive anomaly, signifying a significant increase compared to the normal (**Figure 4(a)**). Conversely, during years of anomalous low biomass burning, May precipitation in the ICP region showed a positive anomaly, indicating a significant increase compared to the normal conditions, while precipitation in southern China showed a negative anomaly, indicating a significant decrease compared to normal (**Figure 4(b)**). In summary, the study reveals that during years of anomalous high biomass burning in the ICP region, the region experiences drought, while southern China experiences flooding. In contrast, during years of anomalous low biomass burning, southern China experiences drought, and the ICP experiences flooding.

The aforementioned analysis results reveal a robust correlation between the anomalous variations of spring biomass burning in the ICP region and May precipitation in southern China. To delve deeper into the potential connection between anomalous biomass burning and abnormal May precipitation in southern China, this study concentrates on scrutinizing the anomalous circulation features linked with biomass burning, such as geopotential height fields, wind fields, and water vapor transport. This scrutiny is essential in gaining an improved comprehension of the plausible linkages between these two factors.

The occurrence of precipitation is dependent upon upward motion. **Figure 5** displays composite fields of 850 hPa geopotential height and wind in May during anomalous spring biomass-burning years in the ICP region. During years of high biomass-burning emissions in the region (**Figure 5(a)**), an elevated geopotential height field emerges over the ICP region, corresponding to a significant westerly wind anomaly. This leads to the strengthening of westerly winds and the

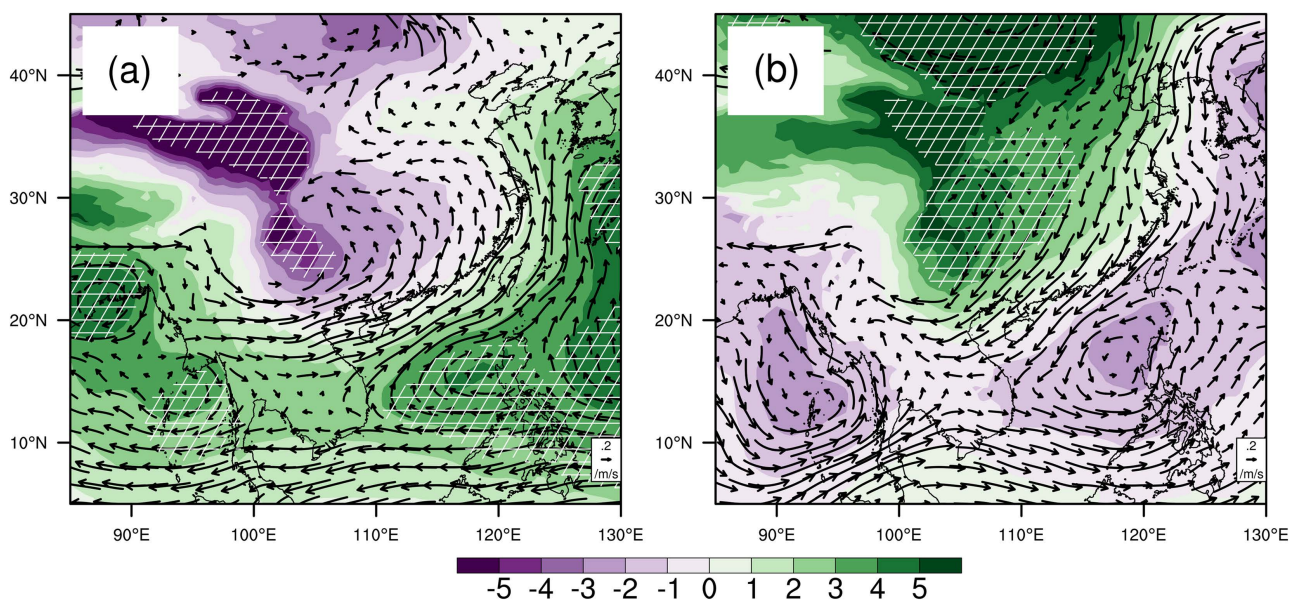


Figure 5. Synthetic fields of May potential height (gpm) and wind field (m/s) distance level: (a) high biomass combustion emission year; (b) low emission year; shaded area passes significance test of 0.05.

weakening of easterly winds, which favors the development of the Asian summer monsoon. However, an anticyclonic circulation anomaly appears over the Bay of Bengal, resulting in a reduction of warm and humid airflow transport from the sea, creating unfavorable precipitation conditions in the ICP region. In southern China, the geopotential height field weakens due to the cyclonic circulation system, leading to an increase in the southwestern wind and a decrease in the northeastern wind. This enhances the transport of warm and humid airflow from the South China Sea, favoring precipitation in the region. During years of low biomass-burning emissions in the region (**Figure 5(b)**), the weakened geopotential height field is mainly located over the sea and the ICP region, where the intersection of warm and humid airflow and cold air favors precipitation occurrence. Furthermore, an anomalous cyclonic circulation over the Bay of Bengal facilitates the transport of warm and humid airflow, providing sufficient moisture for precipitation. The geopotential height field over southern China increases, controlled by the anticyclonic circulation system, resulting in an increase in the northeastern wind and a decrease in the southwestern wind. Strong cold air from the north creates unfavorable precipitation conditions in the region. This circulation pattern partially accounts for the occurrence of drought in the ICP region and floods in southern China during high biomass-burning emission years, as well as the occurrence of floods in the ICP region and drought in southern China during low biomass-burning emission years.

Water vapor plays a crucial role in the formation of precipitation, and a better understanding of this process can be gained through the analysis of the vertically integrated water vapor flux and divergence anomaly composite fields from 1000 to 300 hPa in May, as presented in **Figure 6**. During years of high biomass-burning emissions in the ICP region during spring (**Figure 6(a)**), the water vapor flux

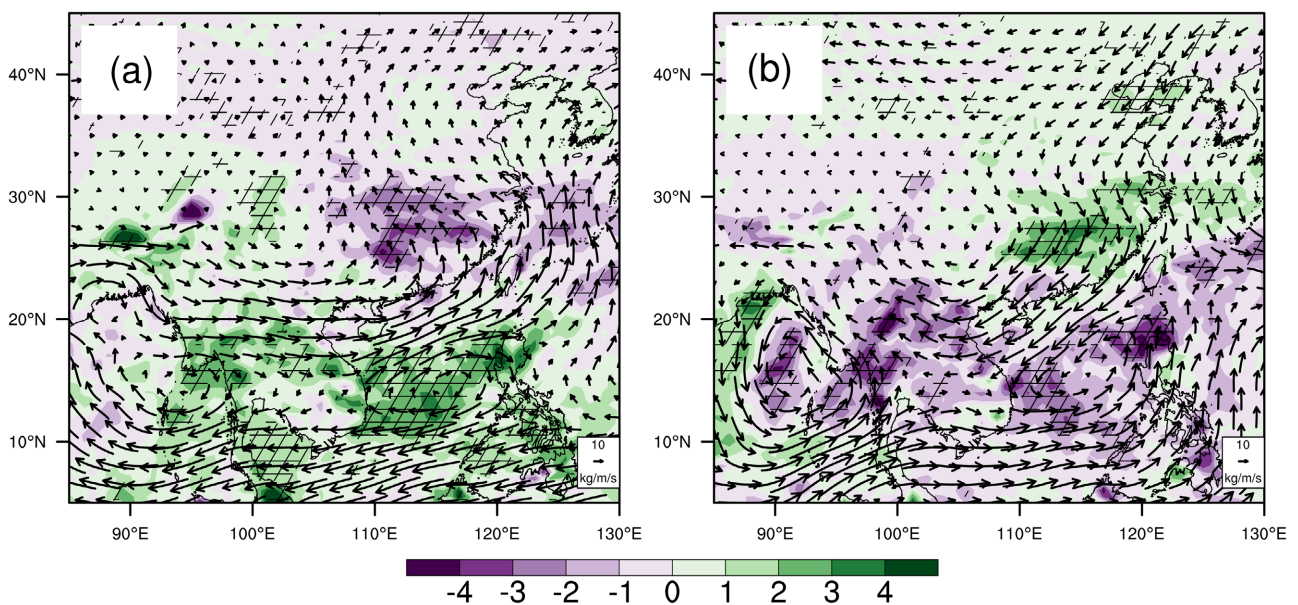


Figure 6. Synthetic fields of water vapor flux ($\text{kg}\cdot\text{m}^{-1}\cdot\text{s}^{-1}$) and dispersion ($10^{-5} \text{ kg}\cdot\text{m}^{-2}\cdot\text{s}^{-1}$) distance levels in May: (a) high biomass combustion emission year; (b) low emission year; shaded area passes significance test of 0.05.

moves predominantly eastward, with a positive water vapor flux divergence indicating a divergent water vapor flux in most parts of the region. On the other hand, in southern China, the water vapor flux moves northeastward from the South China Sea, with a negative water vapor flux divergence indicating a convergent water vapor flux and relatively abundant water vapor conditions. During years of low biomass-burning emissions (**Figure 6(b)**), the water vapor flux in the ICP region moves from the sea to the land, with a negative divergence indicating a convergent water vapor flux and good water vapor conditions that favor precipitation. Meanwhile, the water vapor flux in southern China moves northwestward, with a positive divergence indicating a divergent flux and poor water vapor conditions that are unfavorable for precipitation.

After analyzing circulation patterns and water vapor transport, it was found that high biomass burning in the ICP region during spring leads to cyclonic circulation in the southern China region. This anomalous upward motion, combined with water vapor flux convergence, causes increased precipitation. Conversely, the ICP region is subject to anticyclonic circulation that causes water vapor flux divergence and results in mostly sunny weather, leading to reduced precipitation. Under low emissions, the southern China region experiences abnormal anticyclonic circulation, resulting in poor water vapor conditions, hot and sunny weather, and less precipitation. The ICP region is influenced by cold and warm air currents, which cause anomalous upward motion and good water vapor conditions that lead to increased precipitation in that region.

Based on the aforementioned analysis, it is clear that abnormal circulation patterns during spring in the ICP region correspond to high levels of biomass burning. The onset of the summer monsoon in May results in the suppression of biomass burning in the region, leading to a gradual reduction in emitted aerosols (**Figure 1**). Although the impact of biomass burning is minimal at this stage, its earlier effects on soil moisture are retained for prolonged periods due to its remarkable memory (Shukla and Mintz, 1982). Anomalous soil moisture from previous periods can significantly influence precipitation and temperature for several months into the future. The anomalous atmospheric circulation observed in East Asia during May could be attributed to changes in surface thermal conditions. Biomass burning can result in anomalous precipitation in the ICP region, leading to anomalous soil moisture. Soil moisture is a crucial factor in land-atmosphere interaction and its anomalies can affect surface albedo, heat capacity, vegetation growth, and consequently, the surface energy balance and thermal conditions. Abnormal surface thermal conditions can further affect energy exchange between the land and atmosphere, significantly influencing atmospheric circulation and the monsoon system. Thus, we focus our analysis on the distribution characteristics of anomalous surface temperature and air temperature fields.

During the spring season, the ICP undergoes biomass burning, leading to elevated emissions and a prevalent center of heightened temperature. In contrast, the southern region of China experiences a localized area of decreased surface

temperature. This information is visually presented in **Figure 7(a)**. Conversely, during low-emission years, the central and southern regions of the ICP display a large area of low surface temperature, while northern China has a large area of high surface temperature (**Figure 7(b)**). The distribution of surface temperature indicates that during high-emission years, the early stage of biomass burning suppresses precipitation, causing relatively dry soil moisture content in the area, which, in turn, reduces surface evaporation and leads to decreased soil moisture content and increased surface temperature. Conversely, the opposite occurs during low-emission years. Soil moisture content influences land surface thermal conditions, thereby affecting the energy exchange between the land and the

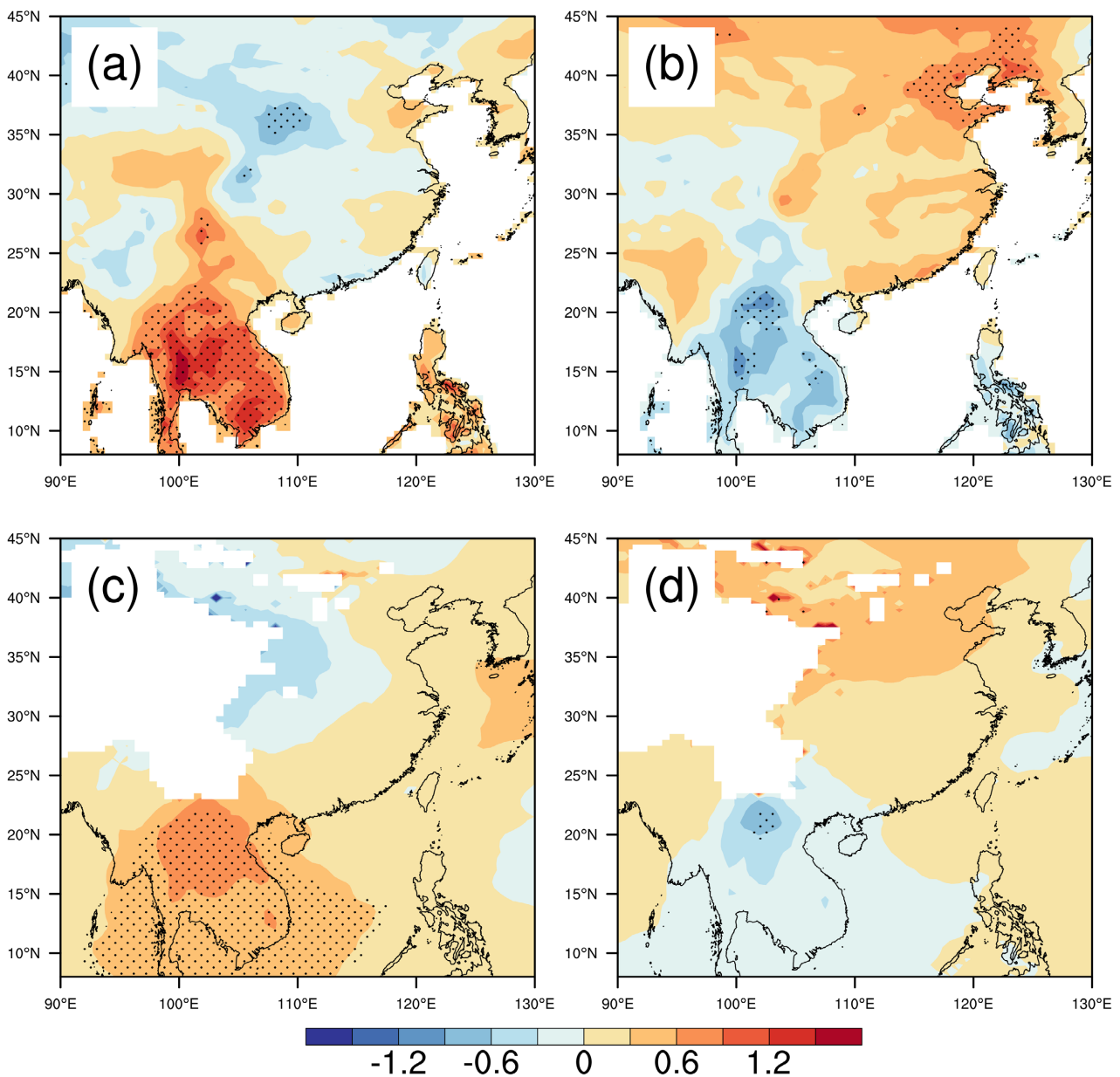


Figure 7. Synthetic field of surface temperature ((a), (b)) and 850 hPa temperature ((c), (d)) distance level in May (unit: K): ((a), (c)) high emission year of biomass combustion; ((b), (d)) low emission year; the punctured area passed the significance test of 0.05.

atmosphere, with higher surface temperature resulting in increased heat transfer from the surface to the atmosphere and lower surface temperature reducing such heat transfer. Analysis of the 850 hPa temperature field reveals that during high-emission years, the temperature in the ICP region deviates positively from the mean value, with only the corresponding high-value center shifting towards the northeast direction with height, consistent with the distribution of surface temperature (Figure 7(c)). The southern region of China also exhibits a weak positive deviation from the mean value, with a relatively large range. During low-emission years, the temperature is low in the central and southern regions of the ICP and high in northern China, consistent with the distribution of surface temperature, with the corresponding high- and low-value centers shifting towards the northeast direction with height. These findings support the notion that changes in soil moisture-induced land surface thermal conditions can affect the atmosphere, as previous studies have shown that abnormal soil moisture content alters land surface thermal conditions, resulting in changes in surface heating that significantly impact atmospheric circulation (Sellers *et al.*, 1997). Therefore, changes in land surface thermal conditions and heating anomalies resulting from these changes may be one of the possible causes of atmospheric circulation anomalies.

4. Summary

This study employs GLDAS-Noah soil moisture data, CPC daily precipitation dataset, and MERRA2 reanalysis data covering the period from 1980 to 2021. By applying a series of statistical methods, this study investigates the spatial distribution features of May precipitation anomalies in southern China and their linkage with anomalous biomass burning occurring in the central and southern peninsulas during the spring season. Furthermore, potential pathways are explored to elucidate how biomass burning in the spring may impact the May precipitation regime in southern China. The main findings of this study are outlined as follows:

- 1) Through statistical analyses of reanalysis data, we have identified significant interannual variability in biomass burning across the central and southern regions of the ICP during the spring season, showing an overall increasing trend. Specifically, the biomass burning tends to be relatively low in the early stages of the season, while it tends to increase in the later stages.

- 2) In the central and southern regions of the ICP during the spring season, biomass burning is found to have a negative correlation with precipitation in May in the same region, but a positive correlation with precipitation in the southern regions of China. In years with high (low) biomass-burning emissions during the spring season in the central and southern regions of the ICP, precipitation tends to be abnormally low (high) in the same region in May, while it tends to be abnormally high (low) in the southern regions of China.

- 3) During years of elevated biomass-burning emissions in the spring season

within the ICP, there are concurrent anomalous subsidence and water vapor flux divergence phenomena that result in abnormally low precipitation levels in the area. In contrast, anomalous upward motion and water vapor flux convergence occur in southern China, leading to unusually high precipitation. Conversely, low emissions during these seasons produce opposite effects.

4) Years marked by heightened biomass-burning emissions during the spring season within the ICP exhibit higher surface temperatures in May, which promote increased heat transfer from the surface to the atmosphere. Conversely, low emissions have the opposite effect. Springtime biomass burning within these regions curtails precipitation, leading to abnormal soil moisture levels. This, in turn, triggers anomalous atmospheric circulation through surface heating changes, ultimately resulting in anomalous precipitation in the southern regions of China during May.

5. Discussion

Adopting a statistical perspective, this study utilized reanalysis data to investigate the relationship between anomalous variations in biomass burning during the spring season in the ICP and May precipitation in southern China. This contributes to an enhanced understanding of the potential correlations between abnormal biomass burning and land-atmosphere interactions, surface energy balance, atmospheric circulation patterns, and precipitation in the region. However, the analysis of the possible physical mechanisms linking these factors in this study is preliminary and solely based on diagnostic analysis of the data. Therefore, further validation is necessary through numerical experiments. Additional research is needed to delve into the underlying physical mechanisms more extensively.

Conflicts of Interest

The authors declare no conflicts of interest regarding the publication of this paper.

References

- [1] Lin, C., Hsu, H., Lee, Y.H., *et al.* (2009) A New Transport Mechanism of Biomass Burning from Indochina as Identified by Modeling Studies. *Atmospheric Chemistry and Physics*, **9**, 7901-7911. <https://doi.org/10.5194/acp-9-7901-2009>
- [2] Akagi, S.K., Yokelson, R.J., Wiedinmyer, C., *et al.* (2010) Emission Factors for Open and Domestic Biomass Burning for Use in Atmospheric Models. *Atmospheric Chemistry and Physics*, **11**, 4039-4072. <https://doi.org/10.5194/acp-11-4039-2011>
- [3] Schwartz, S.E. (1996) The Whitehouse Effect—Shortwave Radiative Forcing of Climate by Anthropogenic Aerosols: An Overview. *Journal of Aerosol Science*, **27**, 359-382. [https://doi.org/10.1016/0021-8502\(95\)00533-1](https://doi.org/10.1016/0021-8502(95)00533-1)
- [4] Hansen, J.E., Sato, M. and Ruedy, R. (1997) Radiative Forcing and Climate Response. *Journal of Geophysical Research*, **102**, 6831-6864. <https://doi.org/10.1029/96JD03436>

- [5] Ackerman, A.S., Toon, O.B., Stevens, D.E., *et al.* (2000) Reduction of Tropical Cloudiness by Soot. *Science (New York, N.Y.)*, **288**, 1042-1047. <https://doi.org/10.1126/science.288.5468.1042>
- [6] Haywood, J.M. and Boucher, O. (2000) Estimates of the Direct and Indirect Radiative Forcing Due to Tropospheric Aerosols: A Review. *Reviews of Geophysics*, **38**, 513-543. <https://doi.org/10.1029/1999RG000078>
- [7] Tao, W., Chen, J., Li, Z., *et al.* (2012) Impact of Aerosols on Convective Clouds and Precipitation. *Reviews of Geophysics*, **50**, RG2001. <https://doi.org/10.1029/2011RG000369>
- [8] Krishnan, R. and Ramanathan, V. (2002) Evidence of Surface Cooling from Absorbing Aerosols. *Geophysical Research Letters*, **29**, 54-1-54-4. <https://doi.org/10.1029/2002GL014687>
- [9] Ding, A.J., Huang, X., Nie, W., *et al.* (2016) Enhanced Haze Pollution by Black Carbon in Megacities in China. *Geophysical Research Letters*, **43**, 2873-2879. <https://doi.org/10.1002/2016GL067745>
- [10] Robock, A. (1988) Enhancement of Surface Cooling Due to Forest Fire Smoke. *Science*, **242**, 911-913. <https://doi.org/10.1126/science.242.4880.911>
- [11] Procopio, A., Artaxo, P., Kaufman, Y.J., *et al.* (2004) Multiyear Analysis of Amazonian Biomass Burning Smoke Radiative Forcing of Climate. *Geophysical Research Letters*, **31**, L03108. <https://doi.org/10.1029/2003GL018646>
- [12] Kolusu, S.R., Marsham, J.H., Mulcahy, J.P., *et al.* (2015) Impacts of Amazonia Biomass Burning Aerosols Assessed from Short-Range Weather Forecasts. *Atmospheric Chemistry and Physics*, **15**, 12251-12266. <https://doi.org/10.5194/acp-15-12251-2015>
- [13] Andreae, M.O., Rosenfeld, D., Artaxo, P., *et al.* (2004) Smoking Rain Clouds over the Amazon. *Science*, **303**, 1337-1342. <https://doi.org/10.1126/science.1092779>
- [14] Koren, I., Kaufman, Y.J., Remer, L.A., *et al.* (2004) Measurement of the Effect of Amazon Smoke on Inhibition of Cloud Formation. *Science*, **303**, 1342-1345. <https://doi.org/10.1126/science.1089424>
- [15] Feingold, G., Jiang, H. and Harrington, J.Y. (2005) On Smoke Suppression of Clouds in Amazonia. *Geophysical Research Letters*, **32**, L02804. <https://doi.org/10.1029/2004GL021369>
- [16] Rosenfeld, D. (1999) TRMM Observed First Direct Evidence of Smoke from Forest Fires Inhibiting Rainfall. *Geophysical Research Letters*, **26**, 3105-3108. <https://doi.org/10.1029/1999GL006066>
- [17] Lau, K.M., Kim, M.K. and Kim, K.M. (2006) Asian Summer Monsoon Anomalies Induced by Aerosol Direct Forcing: The Role of the Tibetan Plateau. *Climate Dynamics*, **26**, 855-864. <https://doi.org/10.1007/s00382-006-0114-z>
- [18] Ding, A., Fu, C., Yang, X., *et al.* (2013) Intense Atmospheric Pollution Modifies Weather: A Case of Mixed Biomass Burning with Fossil Fuel Combustion Pollution in Eastern China. *Atmospheric Chemistry and Physics*, **13**, 10545-10554. <https://doi.org/10.5194/acp-13-10545-2013>
- [19] Lee, D., Sud, Y.C., Oreopoulos, L., *et al.* (2013) Modeling the Influences of Aerosols on Pre-Monsoon Circulation and Rainfall over Southeast Asia. *Atmospheric Chemistry and Physics*, **14**, 6853-6866. <https://doi.org/10.5194/acp-14-6853-2014>
- [20] Huang, X., Ding, A., Liu, L., *et al.* (2016) Effects of Aerosol-Radiation Interaction on Precipitation during Biomass-Burning Season in East China. *Atmospheric Chemistry and Physics*, **16**, 10063-10082. <https://doi.org/10.5194/acp-16-10063-2016>

- [21] Huang, K., Fu, J.S., Hsu, N.C., *et al.* (2013) Impact Assessment of Biomass Burning on Air Quality in Southeast and East Asia during BASE-ASIA. *Atmospheric Environment*, **78**, 291-302. <https://doi.org/10.1016/j.atmosenv.2012.03.048>
- [22] Fang, C., Zhu, B., Pan, C., *et al.* (2020) Regional and Sectoral Sources for Black Carbon over South China in Spring and Their Sensitivity to East Asian Summer Monsoon Onset. *Journal of Geophysical Research: Atmospheres*, **125**, e2020JD033219. <https://doi.org/10.1029/2020JD033219>
- [23] Ramanathan, V., Chung, C., Kim, D., *et al.* (2005) Atmospheric Brown Clouds: Impacts on South Asian Climate and Hydrological Cycle. *Proceedings of the National Academy of Sciences of the United States of America*, **102**, 5326-5333. <https://doi.org/10.1073/pnas.0500656102>
- [24] Bollasina, M.A., Ming, Y. and Ramaswamy, V. (2011) Anthropogenic Aerosols and the Weakening of the South Asian Summer Monsoon. *Science*, **334**, 502-505. <https://doi.org/10.1126/science.1204994>
- [25] Zhang, L., Liao, H. and Li, J. (2010), Impacts of Asian Summer Monsoon on Seasonal and Interannual Variations of Aerosols over Eastern China. *Journal of Geophysical Research*, **115**, D00K05. <https://doi.org/10.1029/2009JD012299>
- [26] Chung, C.E. and Ramanathan, V. (2006) Weakening of North Indian SST Gradients and the Monsoon Rainfall in India and the Sahel. *Journal of Climate*, **19**, 2036-2045. <https://doi.org/10.1175/JCLI3820.1>
- [27] Shi, R.G., Liu, Q.J. and Ma, Z.S. (2015) Numerical Simulation of Aerosol Effects on Cloud and Precipitation Using GRAPES Model. *Meteorological Monthly*, **41**, 272-285.
- [28] Rodell, M., Houser, P.R., Jambor, U., *et al.* (2004) The Global Land Data Assimilation System. *Bulletin of the American Meteorological Society*, **85**, 381-394. <https://doi.org/10.1175/BAMS-85-3-381>
- [29] Schaake, J.C., Koren, V., Duan, Q., *et al.* (1996) Simple Water Balance Model for Estimating Runoff at Different Spatial and Temporal Scales. *Journal of Geophysical Research*, **101**, 7461-7475. <https://doi.org/10.1029/95JD02892>
- [30] Lin, C., Zhao, C., Liu, X., *et al.* (2014) Modelling of Long-Range Transport of Southeast Asia Biomass-Burning Aerosols to Taiwan and Their Radiative Forcings over East Asia. *Tellus B: Chemical and Physical Meteorology*, **66**, Article No. 23733. <https://doi.org/10.3402/tellusb.v66.23733>
- [31] Yu, J., Lin, N., Hsieh, H., *et al.* (2008) A Cluster Analysis of the Springtime Forward Trajectories Arising from Southeast Asia and the Climate Influence. *Journal of Atmospheric Science*, **36**, 287-300.
- [32] Yen, M.C., Peng, C., Chen, T., *et al.* (2013) Climate and Weather Characteristics in Association with the Active Fires in Northern Southeast Asia and Spring Air Pollution in Taiwan during 2010 7-SEAS/Dongsha Experiment. *Atmospheric Environment*, **78**, 35-50. <https://doi.org/10.1016/j.atmosenv.2012.11.015>
- [33] Su, Z., Yacob, A., Wen, J., *et al.* (2003) Assessing Relative Soil Moisture with Remote Sensing Data: Theory, Experimental Validation, and Application to Drought Monitoring over the North China Plain. *Physics and Chemistry of the Earth*, **28**, 89-101. [https://doi.org/10.1016/S1474-7065\(03\)00010-X](https://doi.org/10.1016/S1474-7065(03)00010-X)